

Chandler Wobble Period and Q Derived by Wavelet Transform*

De-Chun Liao and Yong-Hong Zhou

Shanghai Astronomical Observatory, Chinese Academy of Sciences, Shanghai 200030;
ldc@center.shao.ac.cn

National Astronomical Observatories, Chinese Academy of Sciences, Beijing 100012

Received 2003 July 31; accepted 2003 December 1

Abstract We apply complex Morlet wavelet transform to three polar motion data series, and derive quasi-instantaneous periods of the Chandler and annual wobble by differencing the wavelet transform results versus the scale factor, and then find their zero points. The results show that the mean periods of the Chandler (annual) wobble are 430.71 ± 1.07 (365.24 ± 0.11) and 432.71 ± 0.42 (365.23 ± 0.18) mean solar days for the data sets of 1900–2001 and 1940–2001, respectively. The maximum relative variation of the quasi-instantaneous period to the mean of the Chandler wobble is less than 1.5% during 1900–2001 (3%–5% during 1920–1940), and that of the annual wobble is less than 1.6% during 1900–2001. Quasi-instantaneous and mean values of Q are also derived by using the energy density—period profile of the Chandler wobble. An asymptotic value of $Q = 36.7$ is obtained by fitting polynomial of exponential of σ^{-2} to the relationship between Q and σ during 1940–2001.

Key words: polar motion — Chandler wobble — wavelet transform — instantaneous period

1 INTRODUCTION

The two main components in polar motion are the Chandler wobble (CW) and the annual wobble (AW), their amplitudes vary with time and can easily be determined by the least square method from polar motion series. As for the variation of the Chandler period there exist different opinions. Vondrak (1990) classifies these opinions into three categories: (1) there might be several constant proper frequencies of CW; (2) there might be only one frequency of CW and that one varies with time; and (3) there is no sufficient evidence for either of the two opinions above. Besides, some others suggest that the Chandler frequency not only varies with time, but also depends on its amplitudes (Vondrak 1990; Gibert 1998). In the past, spectral analysis methods, such as the Fourier transform, are generally used to investigate the CW. However, the Fourier transform can not reveal the spectral distribution in the time domain. Consequently, when polar motion data series of different duration are used for spectral analysis,

* Supported by the National Natural Science Foundation of China.

some results show that there are several peaks near the Chandler frequency, which mean that the CW have two or more frequencies, while others show that there is only one peak at the Chandler frequency.

The wavelet transform, which has been developed rapidly and applied widely in recent years, can reveal the distribution of the spectral densities in both the frequency and time domain at the same time, therefore, it is suitable for studying time-varying or nonlinear signals. A complex Morlet wavelet function has been defined by Gibert et al. (1998) as

$$\psi^{\pm}\left(\frac{t-b}{a}\right) = \frac{1}{a} \exp\left(-\frac{(t-b)^2}{8a^2\sigma^2}\right) \exp\left(\pm i\pi\frac{(t-b)}{a}\right). \quad (1)$$

It has been used to separate the components of the CW and AW, and then the ridge function is used to find out the instantaneous Chandler frequencies. The real form of the Morlet wavelet,

$$\psi(t) = \exp\left(-\frac{t^2}{2\delta^2}\right) \cos 2\pi\omega t \quad (2)$$

was used by Liu et al. (2000) to construct wavelet function which was used to analyze the X and Y components of polar motion, separately, and then the instantaneous periods and amplitudes of the CW and AW were derived from them. In this study the complex Morlet wavelet in the form of the Eq. (1) is used to analyze the complex form of polar motion ($Z = X - iY$). The advantage of applying the complex wavelet transform is that it avoids the separate analyses for the two components of X and Y which may lead to discrepant results.

2 DATA ANALYSIS

2.1 Data and Pre-processing

Three data series of polar motion are chosen for this study: (1) EOP97C01 (International Earth Rotation Service (IERS) 1997) (1861–2001), a combined polar motion series derived by the IERS. The data are given at 0.1 year intervals prior to 1890. Cubic spline interpolation is used to resample them at 0.05 year intervals as the data became available after 1890. The data series consists of the results of the optical observations prior to 1971, of both optical and modern space geodetic observations (the latter with growing weights year by year during 1972–1987) and of the modern space geodetic observations since 1988. (2) POLE2002 (Gross 2002) (1900–2002), a series at monthly intervals derived by using a Kalman filter to produce a best least squares combination of the optical and modern space geodetic observations by the Jet Propulsion Laboratory (JPL), USA. (3) HIP (1900–1991), a combined solution (Vondrak 1998) of purely optical observations re-produced by using the star positions and proper motions in the HIPPARCS Catalogue system, provided by Dr. J. Vondrak from Czech Republic. The data intervals are nearly at 5-days and are changed to 0.05 year intervals by simple averaging and interpolation in this study. The constant and trend terms in X and Y are removed separately before the complex $Z = X - iY$ (i , the unit of complex) is formed and then analyzed by wavelet transform.

2.2 Wavelet Transform

The wavelet transform of Z is performed using Eq. (1), thus,

$$\begin{aligned} W_{\psi}Z^{\pm}(a, b) &= \frac{1}{\sqrt{a}} \int_{-\infty}^{\infty} Z(t) \overline{\psi^{\pm}\left(\frac{t-b}{a}\right)} dt \\ &= \frac{1}{\sqrt{a}} \int_{-\infty}^{\infty} Z(t) \left\{ \frac{1}{a} \exp\left[-\frac{(t-b)^2}{8a^2\sigma^2}\right] \overline{\exp\left[\pm i\pi\left(\frac{t-b}{a}\right)\right]} \right\} dt. \end{aligned} \quad (3)$$

The results consist of $W_\psi Z^+(a, b)$, the part for positive frequencies, and $W_\psi Z^-(a, b)$, the other part for negative frequencies. The total energy density of the two parts are calculated as

$$|W_\psi Z(a, b)|^2 = |W_\psi^+ Z(a, b)|^2 + |W_\psi^- Z(a, b)|^2. \tag{4}$$

Based on the results obtained by Eq. (4), quasi-instantaneous period of the AW can be derived. However, the quasi-instantaneous period of the CW and Q can only be derived by using the wavelet energy for positive frequencies (i.e., the wavelet energy shown by the first item of right hand side of the Eq. (4)).

2.2.1 Choice of Time Windows

In order to separate and extract the CW and AW components, Gibert et al. (1998) used a control factor $\sigma (= 6)$ in Eq. (1). Considering that there is no need to extract the two components CW and AW, $\sigma = 3$ is also chosen in this study. The time and frequency windows of the complex Morlet wavelet function are shown in Fig.1 for $\sigma = 1, 3$, and 6. It should be noted that in wavelet transform the time windows of the wavelet function vary with the scale factor a . They become narrower when higher frequency signals are analyzed and become wider when lower frequency signals are analyzed. In Fig. 1, A1, A2, and A3 relate to the CW frequency (0.843 cycle per year (cpy) or 433 mean solar days in period), their half amplitude full width (HAFW) of the time windows are about 2.8, 8.3, and 16.7 yrs; B1, B2, and B3 relate to the

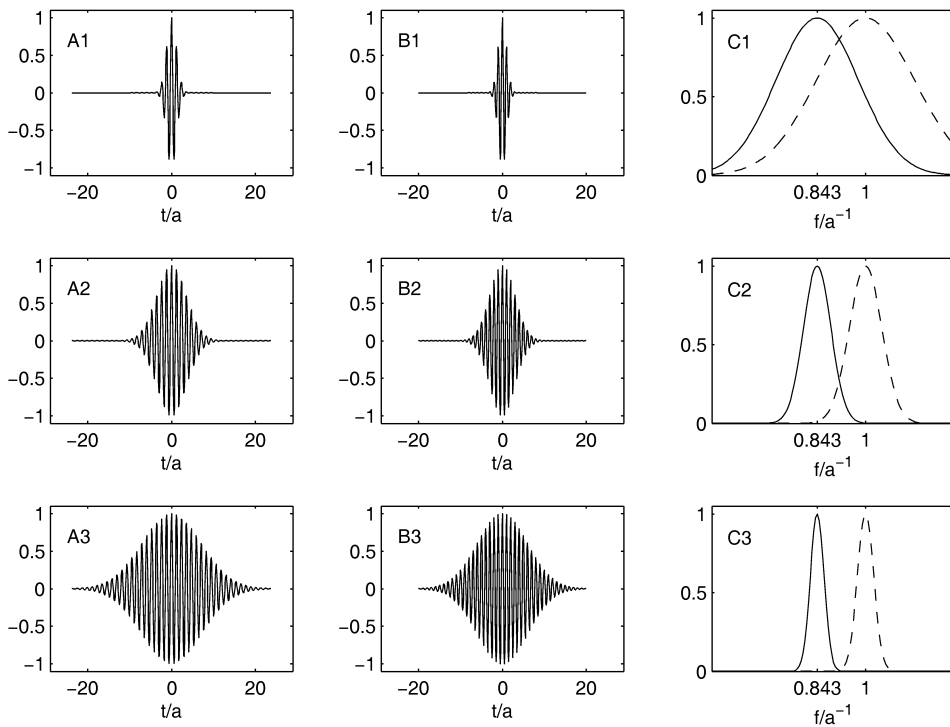


Fig. 1 Time and frequency windows of the complex Morlet wavelet function for $\sigma = 1, 3$, and 6.

AW frequency, their HAFW are about 2.3, 7.0, and 14.0 yrs; C1, C2, and C3 show their frequency windows which are the Fourier transform of their time windows. One can see clearly from the figure that the two frequency windows of the CW and AW are completely separated for $\sigma = 6$ (in C3), so that the two windows can be used to separate and extract the two components; the two windows for $\sigma = 3$ (C2) are mostly separated so that they are sufficient for determining the HAFW of the windows, while the two windows in C1 are mostly overlapping with each other so that they can not be used for our purpose.

2.2.2 Reduction of the Edge-distortion Effect of the Wavelet Transform

As a matter of fact, wavelet transform is a kind of windowed Fourier transform with window width varying with the scale factor (or frequency). Analyses show that the results of wavelet transform, similar to those of other numerical transforms, suffer the effect of edge distortion (Zheng 2000). In order to reduce such effect, a statistical extrapolation was made for each original data series before making the wavelet transform. General procedures of the statistical extrapolation include: (1) the original data series are divided into several independent subseries; (2) the statistical model is fitted and the extrapolation is made by using model parameters for each subseries; (3) a new series is constructed by editing all the extrapolated data points with the original one; (4) the wavelet transform is performed for the new series and then the results are truncated at the two ends so as to have the same length as the original one. In this study the original data series are divided into 6–10 subseries according to the lengths of the data so that each subseries has about 200 points. The auto-regressive (AR(p)) model was chosen for the fitting parameters and for extrapolating the data, the order of the models is about 20 in general and is determined automatically by the criterion of the least final predict errors (FPE) (Akaike 1970).

To reveal the effects of edge distortion of wavelet transform and demonstrate the necessity of reducing the distortion, a comparison of the results of the wavelet transform obtained by using the data with and without statistical extrapolation is shown in Fig. 2, showing contours

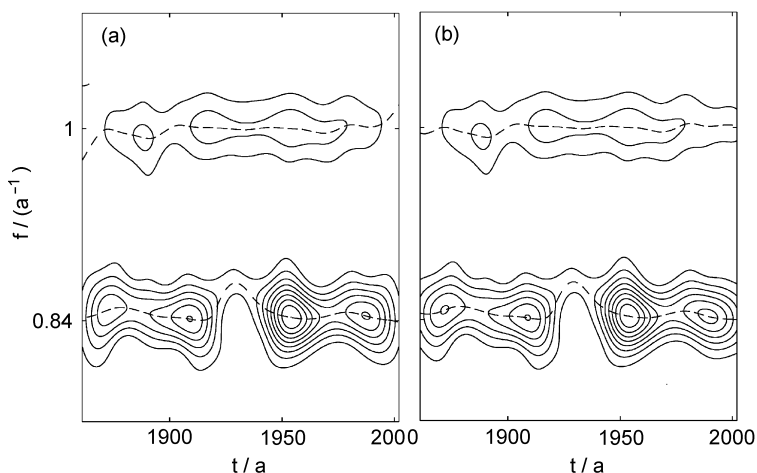


Fig. 2 Comparison of edge distortion of the complex Morlet wavelet transform (a) There appears obvious edge-distortion in the results of the wavelet transform by using original data series; (b) edge-distortion is largely suppressed by using series with statistical extrapolation.

of energy density in the time-frequency plane of the wavelet transform of the IERS polar motion series with $\sigma = 6$. Figure 2a shows the results using the original data series, and Fig. 2b, with extrapolation at the two ends. The two dashed lines mark the instantaneous CW and AW periods. Comparing the parts near the edges in Fig. 2a and Fig. 2b, one can see that the rapid rise and fall in the AW curve at the right and left edges and the fall in the CW curve at both edges seen in Fig. 2a are largely improved in Fig. 2b.

3 RESULTS AND ANALYSES

3.1 Estimates of the Quasi-instantaneous Periods of the CW and AW

The wavelet transform is first performed separately for the data series IERS, JPL, and HIP. Differentiation of the results with respect to frequencies is then made, and lastly the zero points of the differential are identified. The ordinates of these points represent the instantaneous periods of the CW and AW at the moments (the period at each moment is actually derived by analyzing the data in a band pass window, thus it is not really instantaneous but a sort of mean values, that is why we call it quasi-instantaneous period). The results of the quasi-instantaneous periods obtained from the three data series are shown in Fig. 3 for the CW (a, b) and AW (c, d) for $\sigma = 3$ (a, c) and $\sigma = 6$ (b, d), respectively. For comparison, the quasi-instantaneous periods obtained from JPL (HIP) series are added (subtracted) 5 days in the figure. Mean values and their errors of the quasi-instantaneous periods of the CW and AW obtained from each of the different data series in different time periods are listed in Table 1, also listed are the weight mean and their errors of these mean values, together with some results obtained by other researchers.

Table 1 Mean Periods of Chandler Wobble, Annual Wobble and Q , as well as Their Errors

Data series	Duration	Chandler Wobble			Annual Wobble	
		$P_{cw}(\sigma = 3)$	$P_{cw}(\sigma = 6)$	$Q(\sigma = 6)$	$P_{an}(\sigma = 3)$	$P_{an}(\sigma = 6)$
1, PM of EOP97C01	1861–2001	430.53±1.42	431.29±1.32	20.61±0.94	365.36±0.64	365.58±0.32
2, PM of EOP97C01	1900–2001	430.22±1.86	430.31±2.12	19.89±1.18	365.02±0.47	365.26±0.21
3, PM of POLE2002	1900–2002	430.15±1.77	431.04±1.69	20.02±1.16	364.87±0.48	365.06±0.18
4, PM of HIP	1900–1991	429.72±1.92	430.62±1.82	19.84±1.30	365.21±0.49	365.39±0.17
Mean of 1, 3, 4		430.22±0.96	431.06±0.90	20.25±0.64	365.11±0.30	365.28±0.12
Mean of 2, 3, 4		430.04±1.07	430.71±1.07	19.92±0.70	365.03±0.28	365.24±0.11
1, PM of EOP97C01	Ditto with	432.43±0.74	432.64±0.59	20.69±0.94	365.35±0.74	365.61±0.38
2, PM of EOP97C01	data in	432.96±0.73	432.74±0.71	19.83±1.20	364.93±0.53	365.23±0.25
3, PM of POLE2002	1920–1940	432.80±0.69	432.93±0.56	19.81±1.20	364.79±0.54	365.07±0.22
4, PM of HIP	excluded	432.58±0.83	432.65±0.64	19.61±1.32	365.17±0.57	365.33±0.27
Mean of 1, 3, 4		432.61±0.43	432.75±0.34	20.18±0.64	365.05±0.34	365.25±0.16
Mean of 2, 3, 4		432.79±0.43	432.79±0.36	19.76±0.71	364.96±0.31	365.20±0.14
1, PM of EOP97C01	1940–2001	432.63±0.74	432.70±0.74	20.67±1.27	364.98±0.66	365.21±0.32
2, PM of POLE2002	1940–2002	432.55±0.72	432.87±0.67	20.63±1.28	364.92±0.66	365.10±0.29
3, PM of HIP	1940–1991	432.26±0.86	432.50±0.78	20.56±1.48	365.18±0.72	365.40±0.30
Mean of 1, 2, 3		432.50±0.44	432.71±0.42	20.62±0.77	365.02±0.39	365.23±0.18
Liu et al. (2000)	1910–1990		429.78±4.81*		365.72±1.64*	
...	1948–1990		432.82±1.38*		365.42±1.43*	
Vicente & Wilson (1997)	1900–1992		433.1±1.7			
Vondrak (1990)	1976–1988		431.54			
Furuya & Chao (1996)	1983–1994		433.7±1.8	49 (35, 100)		
Wilson & Vicente (1990)	1976–1987		433.0±1.1	179 (74, 789)		
Jeffreys (1968)	1899–1967		433.2±3.4	61 (37, 193)		
Gao Buxi (1990)	1962–1988		436.1	50		
Zhu & Zhou (2001)	1976–1997		433.4 [†]	50 [†]		

* Weight mean of the two estimates listed in Table 1 in Liu et al. (2000);

[†] Mean of the 4 estimates listed in Table 2 in Zhu & Zhou (2001).

It can be seen from Fig.3 that (1) there are larger fluctuations and more details in the quasi-instantaneous periods when $\sigma = 3$ than $\sigma = 6$, and that the CW period showed a rapid fall and rise during 1920–1940. The CW period reached minima of about 408 ($\sigma = 3$) and 419 ($\sigma = 6$) mean solar days, which represent about 3% ($\sigma = 6$) and 5% ($\sigma = 3$) of the relative variations of the quasi-instantaneous periods to the mean periods of the CW; (2) large variations of the quasi-instantaneous AW periods appear in c and d before 1900 which reflect large systematic errors in polar motion data during those early times. Because of this, all the analyses and discussions will be restricted to the results after 1900; (3) the relative variation of the quasi-instantaneous AW period to the mean is less than 1.6% since 1900 (1940), in the same level of the relative variation as of the CW except during 1920–1940.

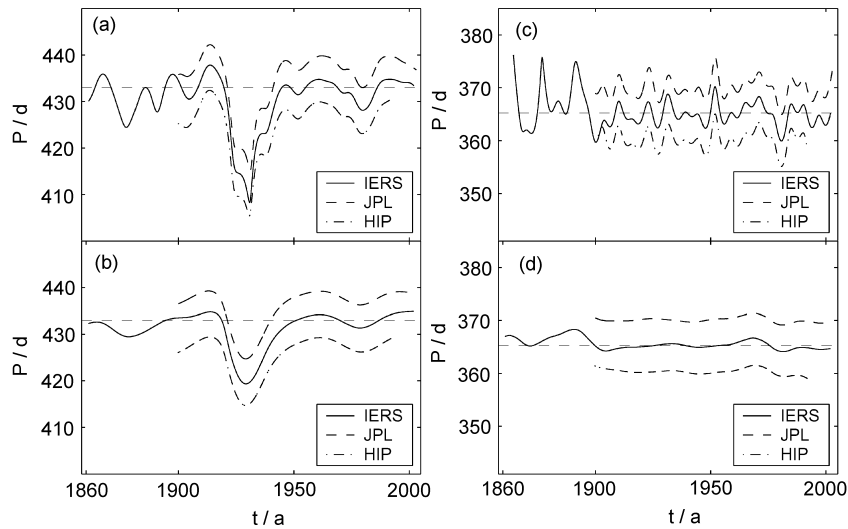


Fig. 3 Comparison of temporal variations of the quasi-instantaneous periods derived from different data series.

It can be seen also from the table that the mean period of the CW (P_{cw}) obtained by using all the data since 1900 are about 2 days smaller than those obtained in the other two cases, and is close to that estimated by Liu et al. (2000). The reason for this is that both in this work and in Liu et al. (2000) the polar motion data in 1920–1940 are included in the analyses of the P_{cw} . When the data during 1920–1940 are excluded or the data from 1940 onwards are used, the estimates of the P_{cw} are obviously close to 433 days which is estimated by previous studies and is accepted by most researchers. In this case the maximum relative variation of the quasi-instantaneous periods relative to the mean P_{cw} is less than 1.5%.

The mean period of the AW (P_{an}) listed in the table are close to the results obtained by Liu et al. (2000), but their error estimates seem to be larger than ours.

3.2 Estimation of Q

Wavelet transform can reveal the energy density distribution of signals in the time-frequency plane. Thus, for any given time epoch, we have an energy density-frequency profile. For

example, Fig. 4 shows such a profile at $t = 2000.0$ for the IERS data series. The two peaks correspond to the energy density distributions in the ranges of frequencies near the CW and AW.

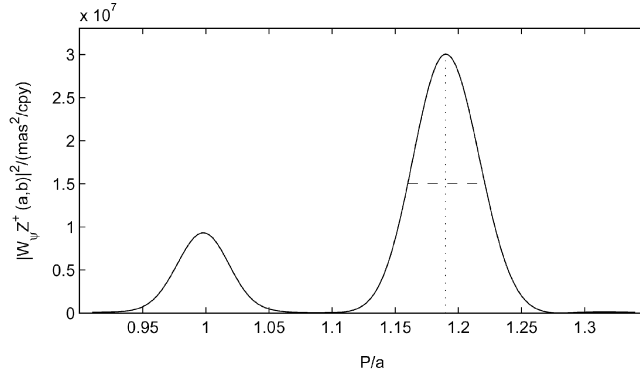


Fig. 4 Example of energy density-frequency profile at a given time.

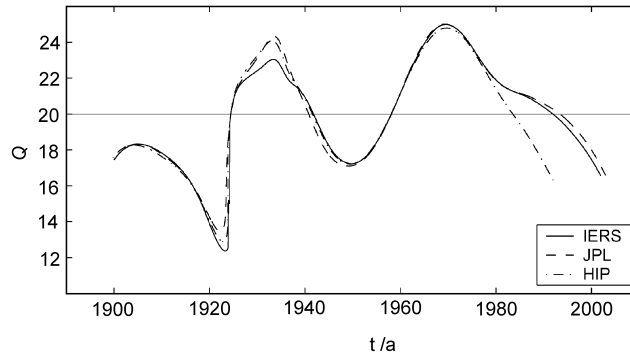


Fig. 5 Comparison of the temporal variation of the quasi-instantaneous Q derived from different data series.

It is well known that the Chandler wobble is a free resonance of the solid Earth. Under the assumption of the solid Earth being a linear resonant body with low damping and low dissipation, the resonant acutance (Munk 1960; Lambeck 1980) is expressed as

$$Q^{-1} = \frac{2\Delta\sigma}{\sigma_0}, \tag{5}$$

where Q is a measure of the dissipation of the solid Earth, σ_0 the resonance frequency and $2\Delta\sigma$ the band width at half power of the spectral peak of the resonance. Using the values of the band width from the energy density profile of Fig. 4 and of the quasi-instantaneous period of the CW derived in Sect. 3.1, the quasi-instantaneous Q can be inferred. The temporal variations of the quasi-instantaneous Q obtained from three polar motion data series for $\sigma = 6$ are shown in Fig. 5. Their mean values and errors are also listed in Table 1, together with some values of Q obtained by previous studies. In comparison with the latter values the Q value obtained in

this work is little smaller. As mentioned in Gao (1990), in order to determine Q precisely using Eq. (5), one needs first to estimate precisely the shape of the peak of the resonant spectrum. In the next section, we will see that the energy density distribution estimated by the wavelet transform, and hence Q , are strongly dependent on the value of σ . The estimated small Q may imply that the energy density—period distribution for $\sigma = 6$ is not the real one near the CW frequency.

A notable feature in Fig. 5 is the departure of the estimated Q value for the HIP series from the other two since 1980s. This is probably due to the lower accuracy of the classical optical observations at the time.

4 VARIATION OF THE QUASI-INSTANTANEOUS MEAN PERIODS AND Q WITH σ

As shown in Fig. 1, the the frequency window of the Morlet wavelet gets narrower when σ takes successively the values 1, 3, and 6, and we even cannot determine the band width at half power of the energy density—period distribution when $\sigma = 3$. This suggests that the energy density—period distribution of the wavelet transform may strongly depend on the values of σ , which will affect the estimates of the periods and Q . The relationships of the quasi-instantaneous periods (Fig. 6a, b) and mean periods (Fig. 6c, d) with σ ($4 \sim 35$) are shown in Fig. 6. The boxes a and c referred to the IERS polar motion data of 1900–2001 and b and d, those of 1940–2001. The correlation between the mean periods and σ in Fig. 6c and Fig. 6d can be described by an exponential as

$$P_m = A_P \exp(B_P \sigma^{-2} + C_P \sigma^{-4} + \dots). \quad (6)$$

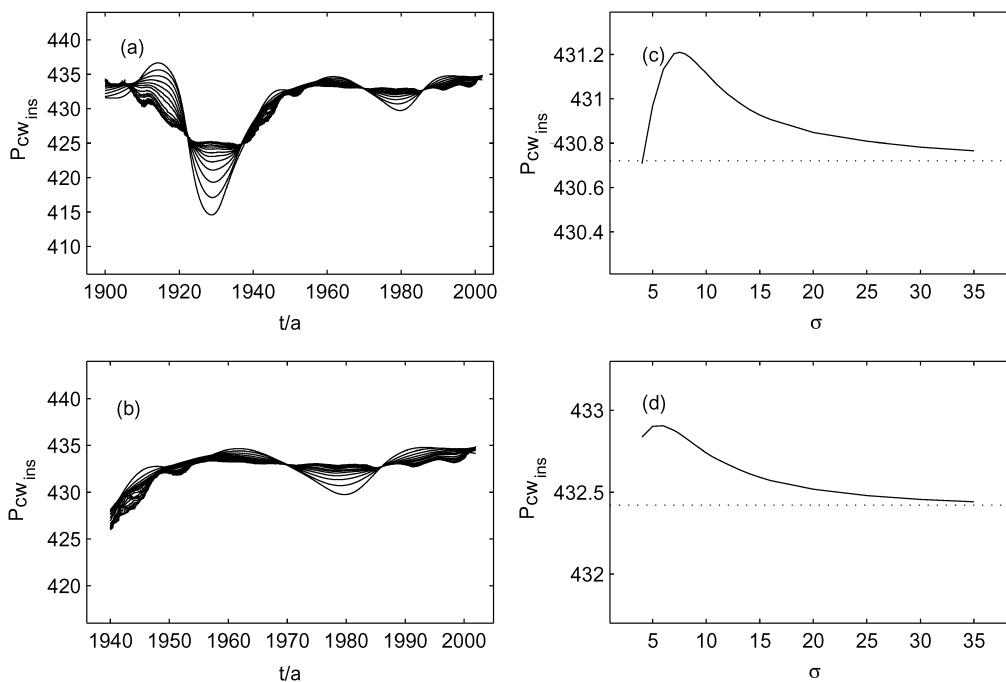


Fig. 6 Variation of quasi-instantaneous and mean periods of the Chandler wobble when using different σ values.

By the least square method, the coefficients A_p , B_p , and C_p, \dots can be obtained. The parameter A_p , called as the asymptotic period in this paper, for 1900–2001 and 1940–2001, are shown by dotted lines in $c(= 430.72 \text{ d})$ and $d(= 432.42 \text{ d})$, respectively, and also listed in Table 2. Those parameters for the results of JPL and HIP polar motion data series are also estimated and listed in Table 2.

Table 2 Asymptotic Periods and Q Fitted from the Correlation of $P_{cw} \sim \sigma$ and $Q \sim \sigma$

	Using data since 1900			Using data since 1940		
	P_{cw}	Q	P_{an}	P_{cw}	Q	P_{an}
IERS	430.72	30.8	365.43	432.42	36.9	365.42
JPL	430.63	30.9	365.37	432.38	36.9	365.31
HIP	430.24	29.9	365.46	432.06	36.4	365.37
Mean	430.53	30.5	365.42	432.29	36.7	365.37

Similarly, the variations of the quasi-instantaneous Q and its mean value with σ are shown in Fig. 7. Coefficients A_q , B_q , and C_q, \dots that describe the correlation between mean Q and σ , are also estimated by using a formula similar to Eq. (6). The parameter A_q , called the asymptotic Q here, is shown by dotted lines in $c(= 30.8)$ and $d(= 36.9)$, and is also listed in Table 2.

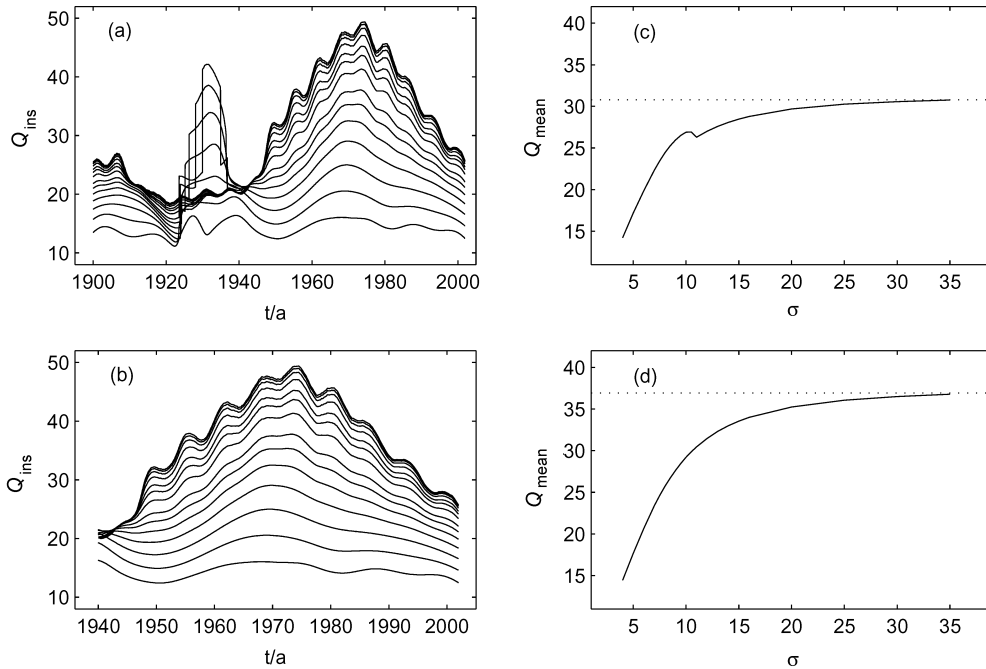


Fig. 7 Variation of quasi-instantaneous and mean Q s of the Chandler wobble when using different σ values.

In Fig. 7(a) there appear strange variations of the quasi-instantaneous Q during 1920–1940. This is due to the complex structure of the energy density — period distribution when σ varies between 4 and 12. The main reason for this is probably the low level of the signal to noise ratio of the Chandler wobble during 1920–1940.

Comparing the periods of the CW (AW) listed in Tables 1 and 2, the asymptotic periods in Table 2 are slightly less (more) than the mean periods in Table 1. However, the differences between them do not exceed the error ranges listed in Table 1. According to the fact that P_{an} ($\sigma = 6$) in Table 1 is closer to the tropical year than the asymptotic one in Table 2, it seems that the mean period P_{cw} ($\sigma = 6$) in Table 1 is better than the asymptotic one in Table 2. As for the estimated Q , the case seems different. A strong exponential correlation between Q and σ has been shown by the large coefficient of B_q which is almost 10 times larger than B_p . Thus the asymptotic Q may be the better one in comparison with the mean Q listed in Table 1.

5 CONCLUSIONS AND DISCUSSION

In this study the quasi-instantaneous and mean periods of the CW and AW are derived from three polar motion data series by means of the complex Morlet wavelet transform. The results show that the mean periods of the CW are 430.7 and 432.7 mean solar days for data series 1900–2001 and 1940–2001, respectively. Relative variation of the quasi-instantaneous periods of the CW to the mean is about 1.5% for 1900–2001 and about 3%–5% for 1920–1940. The estimated Q is 30.5 for 1900–2001, and 36.7 for 1940–2001.

The quasi-instantaneous and mean periods of the AW are also derived. The mean periods of the AW are 365.24 and 365.23 mean solar days for 1900–2001 and 1940–2001, respectively. The relative variation of the quasi-instantaneous periods to the mean is about 1.6% for both data sets.

As for the reason for the large variation of the CW period during 1920–1940, as discussed in Zhao (1988), it is most likely an apparent phenomenon, but not a real change. Theoretically, the free Chandler frequency depends on the ratio $(C-A)/A$ of the principal moments of inertia of the solid Earth, anelastic mantle, oceans and liquid core, etc. Generally, none of these nor the geophysical excitation sources, such as atmosphere, oceans, etc., would vary so much and so fast as to cause a 3%–5% variation in the Chandler frequency. The real feature of the large variation of the CW period is probably that the amplitudes of the CW diminished during 1920–1940, so a small geophysical excitation would cause large phase jumps (even 180 degrees) of the Chandler wobble. Furthermore, large and rapid phase jumps show up as variations of the period in the Fourier transform or other mathematical methods.

Acknowledgements The authors are grateful to the International Earth Rotation Service, to Dr. R. Gross, JPL, USA, to Dr. J. Vondrak, Astronomical Institute, Czech Republic, for providing data series of polar motion, to Prof. Xinhao Liao, SHAO, for his helpful discussion about this work. This study is supported by grants of the National Natural Science Foundation of China under Nos. 10273018, 10133010, and 10373017.

References

- Akaike H., 1970, *Ann. Inst. Math.*, 22, 203
- Furuya M., Chao B. F., 1996, *Geophys. J. Int.* 127, 693
- Gibert D., Holschneider M., Le Mouel J., 1998, *J. Geophys. Res.* 103 (B11), 27069
- Gao B. X., 1990, *Acta Astronomica Sinica*, 31(3), 208
- Gao B. X., 1993, In I. I. Mueller and B. Kolaczek eds., *Developments in astrometry and their impact on astrophysics and geodynamics*. Kluwer Academic Pub., 303
- Gross R. S., 2002, *JPL Publication*, 02-08
- International Earth Rotation Service, 1997 *IERS Annual Report*, Observatoire de Paris. 1998
- Jeffreys H., 1968, *Mon. Not. R. astr. Soc.*, 141, 255
- Lambeck K., 1980, Cambridge: Cambridge Univ. Press
- Liu L. T., Hsu H. T., Gao B. X. et al., 2000, *Geophys. Res. Lett.* 27 (18), 3001
- Munk W. H., MacDonald G. J. F., 1960, Cambridge: Cambridge Univ. Press
- Vicente R. O., Wilson C. R., 1997, *J. Geophys. Res.* 102(B9), 20439
- Vondrak J., 1990, *Bull. Astron. Inst. Czechosl.* 41, 211
- Vondrak J., Pesek I., Ron C., Cepek A., 1998, *Publ. Astron. Inst. Acad. Sci. Czech R.*, 87, 56
- Wilson C. R., Vicente R. O., 1990, In D. D. McCarthy, W. Carter eds., *Variations in Earth Rotation*, *Geophys. Monogr. Ser.*, vol 59, AGU, Washington, DC., 151
- Zheng D. W., Chao B. F., Zhou Y. H. et al., 2000, *J. Geodesy*, 74, 249
- Zhu Y. L., Zhou Y. H., 2001, *Annals of Shanghai Astronomical Observatory*, 22, 26
- Zhao M., 1988, *Sciences in China, Series A*, 7, 741